CD44 Engagement Promotes Matrix-Derived Survival through the CD44-SRC-Integrin Axis in Lipid Rafts[▽][†]

Jia-Lin Lee,[1] Mei-Jung Wang,[1] Putty-Reddy Sudhir,[1] and Jeou-Yuan Chen[1,2*]

Institute of Biomedical Sciences, Academia Sinica, Taipei 11529, Taiwan, Republic of China,[1] and Department of Life Sciences,
National Yang-Ming University, Taipei 11529, Taiwan, Republic of China[2]

CD44 is present in detergent-resistant, cholesterol-rich microdomains, called lipid rafts, in many types of cells. However, the functional significance of CD44 in lipid rafts is still unknown. We have previously demonstrated that osteopontin-mediated engagement of CD44 spliced variant isoforms promotes an extracellular matrix-derived survival signal through integrin activation. By using a series of CD44 mutants and pharmacological inhibitors selectively targeted to various cellular pathways, we show in this study that engagement of CD44 induces lipid raft coalescence to facilitate a CD44-Src-integrin signaling axis in lipid rafts, leading to increased matrix-derived survival. Palmitoylation of the membrane-proximal cysteine residues and carboxyl-terminal linkage to the actin cytoskeleton both contribute to raft targeting of CD44. The enrichment of integrin β1 in lipid rafts is tightly coupled to CD44 ligation-elicited lipid raft reorganization and associated with temporally delayed endocytosis. Through the interaction with the CD44 carboxyl-terminal ankyrin domain, Src is cotranslocated to lipid rafts, where it induces integrin activation via an inside-out mechanism. Collectively, this study demonstrates an important role of the dynamic raft reorganization induced by CD44 clustering in eliciting the matrix-derived survival signal.

The members of the integrin family function as the major cell surface receptors to mediate the interaction and subsequent response of cells with the extracellular matrix (ECM). Evidence has emerged which indicates that changes in integrin subunit composition are critically involved in the development and the homeostasis of multicellular organisms (11). Integrins function as bidirectional transducers of extra- and intracellular signals. The interaction of integrins with their ligands is dependent on signals transduced from the cytoplasmic tails to the extracellular ligand-binding pocket (inside-out signaling), which induces a conformational change and converts the integrin from a low-affinity or "resting" state to a high-affinity or "primed" (also known as "activated") state with increased ligand binding. Binding to ligands, in turn, facilitates the clustering of integrins and leads to an increase in integrin avidity and promotes the transduction of signals to the interior of the cell (outside-in signaling).

The CD44 class I transmembrane glycoproteins are adhesion molecules involved in cell-cell and cell-substrate interactions, including lymphocyte homing and tumor metastasis. CD44 binds to the ECM macromolecule hyaluronan (HA) as well as other glycosaminoglycans including osteopontin (OPN) (29) and collagens and participates in many cellular processes that regulate growth, survival, differentiation, and motility. The *CD44* gene contains 20 exons of which up to 10 variant exons encoding a portion of the ectodomain are alternatively spliced in various combinations, generating numerous CD44 spliced variant isoforms (CD44$_V$) (31). The standard CD44 (CD44$_S$), lacking all variant exons, is

widely expressed in most cell types. The isoform containing sequences from variant exons 8 to 10 (CD44$_E$) is expressed in some epithelial cells. Certain CD44 larger variant isoforms are aberrantly expressed in many human tumors. All CD44 proteins retain the common N-terminal HA-binding 'link' domain, the transmembrane domain, and the C-terminal cytoplasmic tail. The short C tail contains motifs interacting with various proteins, including ERM (for ezrin, radixin, and moesin) proteins that cross-link to the actin cytoskeleton. It is believed that CD44 forms specific protein complexes to monitor changes in the ECM that influence cell growth, survival, and differentiation. Cooperation of CD44 with integrins has been reported in various physiologic and pathological settings. In activated T cells, CD44 can initiate the contact with and mediate subsequent rolling on endothelial cells, and the association of CD44 with integrin VLA-4 (α4β1) assures firm adhesion in the process of immune cell extravasation (22). In breast cancer cells, cross-linking of CD44 induces the expression of VLA-4 and LFA-1 (αLβ2) and increases integrin-mediated adhesion to endothelial cells (40). In chronic myelogenous leukemia, CD44 cooperates with integrin β1 in the regulation of adhesion and proliferation (20). We have also shown that engagement of CD44 promotes integrin activation, leading to an increased matrix survival in transformed cells as well as cells of normal background (17). It is of interest to further define the role of CD44 in integrin activation and the molecular mechanisms involved.

CD44 has been shown to work as a coreceptor modulating the signals emanating from a group of receptor tyrosine kinases, including c-Met and members of the ERBB family (9, 25, 34, 42). Many of the activities that have been ascribed to CD44, in particular those relevant to cancer cell growth, invasion, and metastasis, could be attributed in part to these interactions. Accumulating evidence has shown that many of these receptors and their protein partners are present as large com-

* Corresponding author. Mailing address: Institute of Biomedical Sciences, Academia Sinica, 128 Section 2 Academia Road, Taipei 11529, Taiwan, Republic of China. Phone: 886-2-27899046. Fax: 886-2-27858594. E-mail: bmchen@ibms.sinica.edu.tw.

plexes, which might involve lipid rafts (9, 23, 38). The ligand-induced translocation of receptors into discrete microdomains in the plasma membrane that concentrate essential components of the signaling pathway represents a previously unappreciated step in signal transduction. The role of lipid rafts has been well described in immune cell activation. Upon ligand binding, the multichain immune recognition receptors are translocated into rafts, where they are phosphorylated to form highly ordered, polarized immunological synapses (6). A variety of important glycosylphosphatidylinositol-linked immune cell surface proteins are assembled in membrane microdomains upon cross-linking to initiate signaling in T-cell proliferation and functional differentiation (10). Recently, several studies have highlighted the possibility that HA binding induces redistribution of CD44 into lipid rafts, with multiple signal molecules being recruited and assembled to facilitate the transduction of signals (7, 9, 13). To dissect the role of CD44 in integrin-mediated cellular functions, in this study, we tested whether CD44, a temporary raft-residing protein, may act as a scaffold to elicit the establishment of a specific signaling platform in lipid rafts to ensure efficient and sustained signal transduction. We show that engagement of CD44 induces lateral reorganization of lipids and membrane-associated proteins, with CD44, Src, and integrin β1 enriched in lipid rafts, and with the assembly and activation of an integrative CD44-Src-intergin β1 signaling complex leading to increased cell-matrix interactions.

MATERIALS AND METHODS

Antibodies and reagents. The hybridoma for Hermes-3 (H-3) was from the American Type Culture Collection (ATCC, Manassas, VA). Antibodies for integrin β1 (P4C10 for the blocking experiment and HUTS-4 for detecting the active form of β1 integrin by Western blotting) were from Chemicon (Temecula, CA). The monoclonal antibody (MAb) HUTS-21 for detecting activated β1 integrin by flow cytometry and the anti-FAK antibody (Ab) were from BD Biosciences Pharmingen (San Diego, CA). Antibodies for caveolin-1, Erk2, flotillin-2, and ezrin were from Santa Cruz Biotechnology (Santa Cruz, CA). The Ab for the transferring receptor was from Zymed Laboratories (San Francisco, CA). The Ab for c-Src was from Upstate (Lake Placid, NY). The Ab for Akt was from Cell Signaling Technology (Danvers, MA). The Ab for Src-pY418 was from Biosource (Camarillo, CA). PP2, LY294002, wortmannin, PD98059, and GF109203X were from Calbiochem (San Diego, CA). Nystatin, curcumin, and methyl-β-cyclodextrin were from Sigma-Aldrich (St. Louis, MO). Alexa 488- and Alexa 594-conjugated anti-mouse or anti-rabbit immunoglobulin G (IgG) were obtained from Molecular Probes (Eugene, OR). Preparation and purification of OPN has been described previously (17).

Constructs, cell culture, and transfection. Human gastric adenocarcinoma AZ521 and colorectal cancer HT29 cell lines were from American Type Culture Collection. The temperature-sensitive v-Src-transformed MDCK cell line was kindly provided by Jürgen Behrens (Department of Cancer Biology, Max-Delbrück-Center for Molecular Medicine, Berlin, Germany) (1). The construction of expression vectors pcDNA-CD44$_S$, pcDNA-CD44$_E$, and pcDNA-CD44$_{V6-10}$ has been previously described (17). The CD44$_S$ mutants with C-terminal deletions (Δ37, Δ61, and Δ67) were generated by PCR amplification of the corresponding cDNA fragments using the wild-type CD44$_S$ as a template. The CD44 cysteine mutants (C286A and/or C295A) and the lysine-to-alanine (KA) mutant were generated by site-directed mutagenesis using the wild-type CD44$_S$ as a template. The correct sequence of the clones was verified by sequencing. The vectors encoding FAK(Y397F) and Src(K297D) have been described previously (17). AZ521/Mock and AZ521/CD44 cell clones were established by transfection of AZ521 cells with pcDNA-3-myc and the respective pcDNA-CD44 plasmids by the electroporation method followed by selection of G418-resistant clones as described previously (3). Transient transfection was performed using the Lipofectamine 2000 reagent (Invitrogen Corp., Carlsbad, CA) according to the manufacturer's protocol. Engagement of CD44 was performed by incubating cells precultured in serum-free medium for 24 h in the same medium containing H-3

(20 μg/ml) or OPN (10 μg/ml) at 37°C for 1 h or as indicated. For methyl-β-cyclodextrin (MβCD) treatment, cells were preincubated with 5 mM MβCD for 15 min at 37°C prior to H-3 treatment.

Lipid raft isolation. Cells were scraped in 1% cold Triton X-100 buffer (10 mM Tris-HCl, pH 7.4, 150 mM NaCl, 1% Triton X-100, 1% deoxycholate, 0.1% sodium dodecyl sulfate [SDS], 1 mM EGTA, 10 μg/ml leupeptin, 10 μg/ml aprotinin, 1 mM phenylmethylsulfonyl fluoride, and 1 mM sodium orthovanadate) and lysed on ice for 30 min. After centrifugation at $800 \times g$ to remove nuclei and cell debris, lysates were subjected to sucrose gradient fractionation as described previously (39). An equal volume of each fraction was boiled in SDS-Lammeli sample buffer and electrophoresed on a 10% SDS-polyacrylamide gel followed by immunoblotting analyses as described previously (16). Alternatively, the Triton-insoluble rafts and Triton-soluble fractions were diluted with an equal volume of extraction buffer (25 mM HEPES, pH 7.6, 0.3 M NaCl, 1.5 mM MgCl$_2$, 0.2 mM EDTA, 1% Nonidet P-40, and 0.5 mM dithiothreitol) and subjected to immunoprecipitation as described previously (16).

Lentiviral preparation, viral infection, and stable cell generation. A pLKO.1-shRNA plasmid encoding a short hairpin RNA (shRNA) with scramble sequences or sequences targeting human *Src*, purchased from the National RNAi Core Facility, Taiwan, was introduced into HEK293T cells with lentiviral packaging vectors pMD.G and pCMVΔ8.91. The shRNA sequence targeting human *Src* contains 5′-CCG GGT CAT GAA GAA GCT GAG GCA TCT CGA GAT GCC TCA GCT TCT TCA TGA CTT TTT G-3′, with underlined sequences corresponding to positions 946 to 966 relative to the first nucleotide of the start codon. Viruses were collected from the medium 60 h after transfection. For knockdown experiments, HT29 cells were infected with the collected viruses over 24 h in the presence of Polybrene, followed by selection in medium containing puromycin (2 μg/ml) for 7 to 9 days. To reexpress a functional Src, a plasmid containing a "wobble" mutant cDNA encoding mouse *Src* with synonymous point mutations within the shRNA target sequence (5′-GTT ATG AAA AAA TTA CGC CAC-3′, with mutation sites underlined) was constructed and transfected into HT29 cell clones harboring the shRNA-*Src*.

Immunoprecipitation and immunoblot analysis. Total cell lysates were prepared by lysing cells in 25 mM HEPES (pH 7.6), 0.3 M NaCl, 1.5 mM MgCl$_2$, 0.2 mM EDTA, 1% Nonidet P-40, and 0.5 mM dithiothreitol. For immunoprecipitation, the cell extracts (1 mg total proteins) were precleaned by rotation for 1 h with 20 μl of protein G-Sepharose beads (Santa Cruz, CA). The precleaned supernatant was incubated with anti-CD44 MAb H-3 overnight. After incubation with 20 μl of protein G-Sepharose beads for 1 h, the suspension was centrifuged and pellets washed and collected as immunoprecipitation complexes.

Western blotting was performed as previously described (17). Images were recorded using a Fuji LAS-3000 luminescent image analyzer, and the intensities of the bands were quantitated by densitometry (Multi Gauge v. 3.0 software; FujiFilm Life Science, Tokyo, Japan).

Immunocytostaining. Cells were fixed in 4% paraformaldehyde, incubated consecutively with primary Ab and Alexa 594- or Alexa 488-conjugated secondary Ab, counterstained with 4′,6-diamidino-2-phenylindole-dihydrochloride (DAPI), and examined under a laser-scanning confocal system (MRC 1000; Bio-Rad, Hercules, CA). Image J software (National Institutes of Health) was used to process the immunocytostaining signals of CD44 and the raft marker (caveolin-1) for colocalization.

Flow cytometric analysis. Flow cytometric analysis was as previously described (17). Cells were trypsinized, fixed, stained with MAb HUTS-21 or an isotype IgG, labeled with Alexa 488-conjugated secondary Ab, and subjected to flow cytometric analysis using a FACSCalibur (BD Biosciences). Cells were not fixed while assessing cell surface expression. The specific fluorescence index was calculated as the ratio of the mean fluorescence values obtained with the specific anti-specific Ab and the isotype control Ab.

Adhesion assay. The adhesion assay was performed as previously described (16, 17). Adhesion of cells to plates coated with 10 ng/μl of fibronectin (FN), 2 mg/ml of poly-D-lysine, or 1% bovine serum albumin in phosphate-buffered saline (PBS) was assessed. For Mn^{2+}-induced adhesion, 2 mM MnCl$_2$ was added to the cell suspension before adhesion assays. In some experiments, cells were preincubated with 5 μg/ml of blocking (anti-integrin β1) Ab for 1 h at 37°C and subjected to adhesion assays. The reference value for 100% attachment was obtained by seeding cells on plates precoated with 20 ng/μl FN; cells were incubated for 3 h at 37°C under tissue culture conditions followed by immediate fixation, and ~90 to 100% of input cells were recovered.

Apoptosis assay. Apoptosis assay was as previously described (17). After UV irradiation, cells were harvested at designated times, stained with propidium iodide, and subjected to flow cytometric analysis of sub-G$_1$ apoptotic fractions. Alternatively, cells were subjected to annexin V staining for apoptotic fractions using an Annexin-V-FLUOS staining kit (Roche, Mannheim, Germany) and
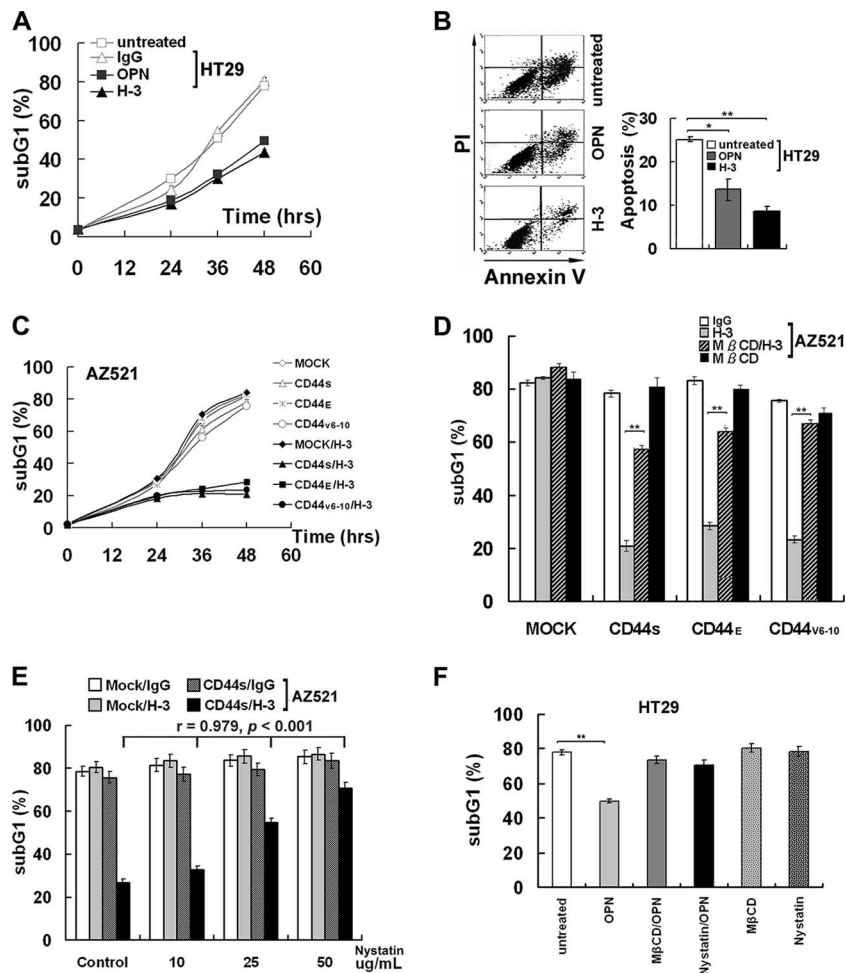
FIG. 1. Engagement of CD44 leads to an increased resistance to apoptosis which is dependent on lipid raft reorganization. HT29 (A, B, and F) and AZ521 (Mock, CD44$_S$, CD44$_E$, and CD44$_{V6-10}$) (C to E) cells were cultured in serum-free medium for 24 h, treated with or without OPN, H-3 MAb, or control IgG for 30 min, irradiated with UV at 90 J/m^2, and incubated for a designated time prior to apoptosis assays by flow cytometric analyses (in panels A and C to F) and annexin V staining (in panel B). For treatment of lipid raft-destabilizing drugs, cells were pretreated with or without 5 mM MβCD for 15 min (in panels D and F) and with increasing concentrations of nystatin (0, 10, 25, and 50 μg/ml) (in panel E) or 50 μg/ml of nystatin (F) for 30 min prior to the incubation with H-3 MAb or control IgG, and cells were harvested for flow cytometric analysis 48 h after UV treatment. Data were derived from three separate experiments. In panels B, D, and F, means ± standard deviations and t test results are shown. ∗, $P < 0.05$; ∗∗, $P < 0.01$. In panel E, Pearson's correlation coefficients were measured for the effects of increasing dosages of nystatin.

analyzed with a FACSCalibur. To test the role of integrins, cells with or without CD44 engagement were replated on FN- or poly-D-lysine-coated dishes for 3 h. Cells were UV irradiated and harvested within 48 h for flow cytometric analysis. Alternatively, cells were pretreated with blocking Ab against integrin β1 for 1 h at 37°C prior to CD44 Ab-mediated engagement.

Receptor internalization assay. AZ521/CD44$_S$ cells cultured to 70 to 80% confluence were briefly washed on ice with ice-cold PBS, and then N-hydroxy-succinimide-biotin (1.0-mg/10-ml/10-cm dishes; Pierce, Rockford, IL) was added. The cells were then incubated with gentle agitation for 60 min at 4°C. Cells were incubated with control IgG or H-3 for 30, 60, and 240 min at 37°C (with serum), further incubated with 0.1 M glycine in PBS for 30 min at 4°C (to quench any unreacted biotin before lysis), and lysed in lysis buffer. Biotinylated proteins were precipitated using streptavidin beads from equal amounts of cell lysates. The amounts of receptor bound to beads were determined by immunoblotting.

RESULTS

Engagement of CD44 leads to an increased resistance to apoptosis which is dependent on lipid raft reorganization. Engagement of CD44 was initiated by treating the subconflu-

ent colon HT29 cells, which express high levels of endogenous CD44$_S$ and other variant isoforms, with physiologic ligand OPN or with anti-pan CD44 MAb H-3. OPN binds and induces ligation of CD44 isoforms expressing either of the variant exon 6- or 7-encoded sequences, whereas H-3 induces ligation of all isoforms of CD44. As shown, engagement of CD44 by OPN or H-3 MAb-conferred cells increased survival against UV-induced apoptosis measured by flow cytometric analysis (Fig. 1A) and by annexin V staining (Fig. 1B). We have also established cell clones expressing various CD44 isoforms in AZ521 cells that expressed endogenous CD44 at an undetectable level. As shown, MAb-mediated cross-linking of CD44 significantly suppressed UV-induced apoptosis in the AZ521 (CD44$_S$, CD44$_E$, and CD44$_{V6-10}$) cell clones but not in the AZ521/Mock cells (Fig. 1C). When the AZ521 cell clones were treated with OPN, CD44 ligation induced anti-apoptosis in AZ521/CD44$_{V6-10}$ cells but not in AZ521/Mock, CD44$_S$, and

CD44$_E$ cells (see Fig. S1 in the supplemental material). CD44 has been shown as one of the temporary raft-resident proteins (7, 12, 24, 28). To examine whether the formation of intact lipid rafts is required for CD44-mediated survival, cells were treated with lipid raft-destabilizing drugs, MβCD or nystatin, prior to cross-linking of CD44. Our data showed that inhibition of raft formation by MβCD or nystatin abolished CD44-mediated survival, and a dose-dependent inhibition by nystatin was shown (Fig. 1D and E). Similarly, anti-apoptosis induced by OPN-mediated ligation of endogenous CD44 was also abrogated when HT29 cells were pretreated with MβCD or nystatin (Fig. 1F).

CD44 engagement induces lipid raft coalescence and promotes the enrichment of CD44, Src, and integrin β1 into lipid rafts. We then examined the localization of CD44 in lipid rafts upon CD44 engagement. As shown, engagement of CD44 by OPN or CD44 MAb (H-3) induces redistribution of both the ectopically (in AZ521) and endogenously (in HT29) expressed CD44 to be colocalized with raft marker caveolin-1 (Fig. 2A). In comparison, the untreated or IgG-treated cells were without patching of CD44. A quantitative assessment revealed that a significantly higher percentage of engaged CD44, compared to the untreated, was colocalized with the lipid raft marker. Most importantly, this association was severely blocked by the treatment of MβCD. In agreement, we also showed that ligation of CD44 by OPN promoted the association of CD44 and caveolin-1 in AZ521/CD44$_{V6-10}$ and HT29 cells by coimmunoprecipitation and that OPN-elicited complex formation between CD44 and caveolin-1 was inhibited by MβCD (Fig. 2B). We next examined the distribution of CD44 in lipid rafts by solubilizing AZ521/CD44$_{V6-10}$ cells in 1% cold Triton X-100 solution followed by sucrose gradient centrifugation. The lipid rafts were recovered from the low-density buoyant fractions, as indicated by the presence of caveolin-1 and flotillin-2, whereas the Triton X-100-soluble cellular components were distributed over fractions 7 to 10, where the transferrin receptor was recovered. As shown, engagement of CD44 greatly enhanced the translocation of CD44 into lipid rafts (Fig. 2C). CD44 engagement induced a lateral redistribution of transmembrane proteins and membrane-associated proteins into lipid rafts, as demonstrated by the increased amount of proteins (nearly by threefold) recovered from the low-density raft fractions (pooled from fractions 2 to 4) (see Fig. S2 in the supplemental material). We further studied the dynamic changes in protein profiles in lipid rafts upon CD44 engagement. We particularly wanted to identify proteins that are associated with CD44. Raft fractions were prepared from AZ521/CD44$_S$ cells, pooled, and immunoprecipitated using anti-CD44 Ab. The immunoprecipitated proteins were separated by SDS-polyacrylamide gel electrophoresis (PAGE) and visualized by silver staining (Fig. 2D). The protein bands were excised from the gel, digested by trypsin, and subjected to liquid chromatography-tandem mass spectrometry analysis. The proteins that were identified to be associated with CD44 in lipid rafts include integrin β1, ezrin, Src, and actin. Engagement-induced lateral redistribution of CD44 into lipid rafts was clearly observed as early as 30 min after Ab-mediated cross-linking (with a concomitant enrichment of integrin β1 and Src in rafts), reached a plateau at 2 h, and progressively declined after 4 h (Fig. 2E). In contrast,

FAK, Erk, and Akt remained in the detergent-soluble fractions.

Both palmitoylation and linkage to the actin cytoskeleton contribute to raft targeting of CD44. CD44 has been shown to be palmitoylated through thioacylation at the membrane-proximal cysteine residues; this is essential for the association with lipid rafts (19, 36). We generated a palmitoylation-deficient mutant by changing the predominant thioester sites present in CD44 (Cys^{286} and Cys^{295}) to alanine, and we explored the association of the palmitoylation-deficient CD44 with lipid rafts. As shown in Fig. 3A, the removal of these acylation sites did not prevent the relocalization of the resultant CD44 (CD44$_S^{C286A}$, CD44$_S^{C295A}$, and CD44$_S^{C286,295A}$) in the raft fractions upon receptor engagement. We then tested whether the C-terminal tail of CD44 contributes to raft affinity through interaction with cellular proteins. A series of C-terminal deletion mutants were generated from the wild type as well as the cysteine mutant. Progressional deletion of most of the entire 70-amino acid (aa) C-terminal tail did not block the association of the wild type and most of the palmitoylation-deficient mutants with lipid rafts. As demonstrated, CD44$_S$Δ67 (Δ67, deletion of aa 295 to 361) and CD44$_S$Δ61^{C286,295A} (Δ61, deletion of aa 301 to 361) were still recovered from the low-density raft fractions upon CD44 engagement. It was only when the only membrane-proximal cysteine residue was abolished in the CD44$_S$Δ67 mutant that the resultant CD44$_S$Δ67^{C286A} mutant was no longer associated with lipid rafts, suggesting that both palmitoylation and C-terminal protein-protein interactions contribute to CD44 raft targeting. In the comparison of amino acid sequences of raft-targeting CD44$_S$Δ61^{C286,295A} and non-raft-targeting CD44$_S$Δ67^{C286A}, a protein 4.1, ezrin, radixin, and moesin (FERM)-binding motif was identified located in the C-terminal region within aa 292 to 300 (18). The ERM family proteins can function to cross-link transmembrane receptors, including CD44, to actin-based cytoskeletons (37). To corroborate whether CD44 is associated with lipid rafts via linkage to the actin cytoskeleton, the FERM-binding motif in CD44$_S$Δ61^{C286,295A} was mutated from ^{292}RRRCGQKKK^{300} to ^{292}RRRCGQAAA^{300} (mutated amino acids are underlined). As shown in Fig. 3A, the resultant CD44$_S$Δ61$^{C286,295A/KA}$ mutant was no longer associated with lipid rafts. We also showed that engagement of CD44 mutants that were defective in association with lipid rafts failed to induce lipid raft reorganization (see Fig. S3 in the supplemental material). Consistent with the notion that linkage to the actin cytoskeleton also promoted the association of CD44 with lipid rafts, depolymerization of actin microfilaments by treating cells with cytochalasin D prior to H-3 MAb stimulation significantly blocked the association of the palmitoylation-deficient mutant with rafts. As shown, only a background level of CD44$_S^{C286,295A}$ was observed in lipid rafts, whereas the association of palmitoylation-proficient wild-type CD44 to rafts was not affected (Fig. 3B). In contrast, treating the cells with inhibitors selectively targeted at Src (PP2), PI-3 kinase (LY294002 and wortmannin), mitogen-activated protein kinase (PD98059), protein kinase C (GF109203X), and NF-κB (curcumin) had little effect on the apparent association of palmitoylation-proficient or -deficient CD44 with rafts. The blockage of the association of the palmitoylation-deficient mutant with rafts was accompanied by the diminished association of β-actin with rafts upon cytochalasin D treatment (Fig. 3C). Coimmunoprecipitation assays indicated that deletion of the
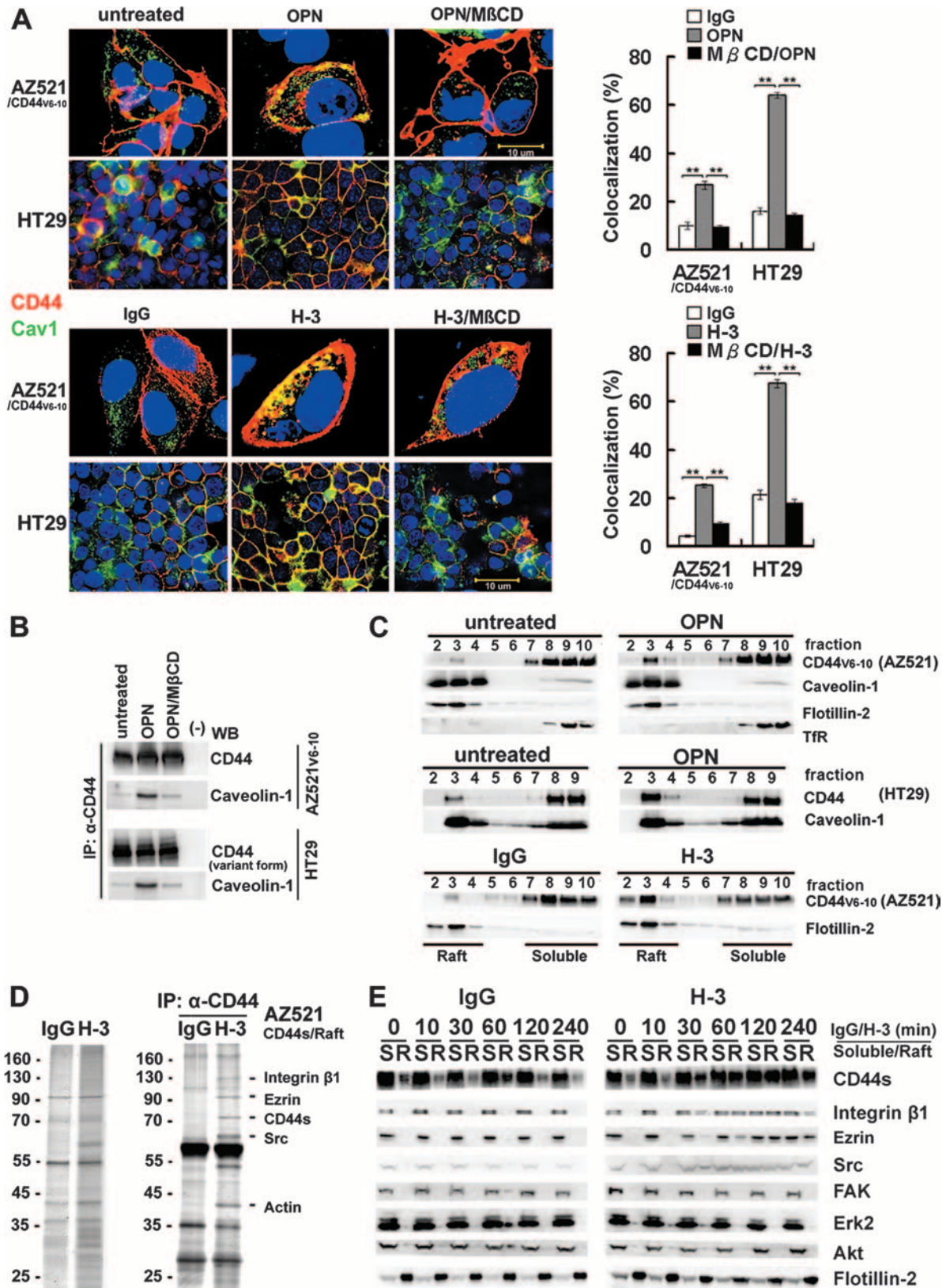
FIG. 2. Engagement of CD44 induces relocalization of CD44, Src, and integrin β1 to lipid rafts. (A) Immunofluorescence examination of CD44 and raft marker in AZ521/CD44$_{V6-10}$ and HT29 cells treated with or without OPN or H-3. For staining of CD44, cells were incubated with H-3 (20 µg/ml) for 1 h followed by fixation and labeling with Alexa 594-conjugated secondary Ab, whereas the control and OPN (10 µg/ml)-treated cells were fixed and incubated with H-3 MAb followed by labeling with Alexa 594-conjugated anti-mouse IgG. Both the stimulated and control

FERM-binding domain (as $CD44_S\Delta67$ and $CD44_S\Delta67^{C286A}$) or mutation of this motif (as $CD44_S\Delta61^{C286,295A/KA}$) disrupted the association of CD44 with ezrin and actin (Fig. 3D). On the other hand, CD44 proteins containing an intact FERM domain, including $CD44_S$, $CD44_S\Delta37^{C286,295A}$, and $CD44_S^{C286,295A}$, were constantly associated with actin and ezrin, and engagement of CD44 strongly enhanced the formation of the CD44-ezrin-actin complex (Fig. 3D).

CD44-mediated survival signaling is dependent on integrin activation in lipid rafts. We have previously shown that OPN-$CD44_V$ interaction confers to cells an increased survival mediated through a Src-dependent inside-out mechanism leading to integrin activation (17). Based on the findings that CD44-mediated survival is dependent on raft reorganization, we further addressed the involvement of lipid raft reorganization in these processes. To test the role of integrin activation involved in CD44-mediated survival, we showed that engagement of CD44 efficiently suppressed UV-induced apoptotic response in the AZ521 cell clones expressing CD44 when plated on FN but not in the control cells and that pretreatment of cells with blocking Ab against integrin β1 significantly blocked CD44-mediated anti-apoptosis (Fig. 4A). Most importantly, we showed that MβCD treatment significantly blocked integrin activation elicited by either H-3-induced cross-linking of CD44 in $AZ521/CD44_S$ cells or OPN-mediated ligation of endogenous CD44 in HT29 cells (Fig. 4B). To further elaborate the involvement of lipid raft reorganization in CD44-elicited integrin activation, we examined integrin activation in Triton X-100-soluble and -insoluble fractions upon CD44 engagement. Integrins were present mainly in the detergent-soluble cytosolic fraction in an inactive state in unstimulated cells. Upon engagement of CD44, they were present in both detergent-soluble and -insoluble fractions, and it was noted that the activated integrins were only detected in the raft fraction (Fig. 4C). We further showed that the engagement of CD44 mutants such as $CD44_S\Delta67^{C286A}$ and $CD44_S\Delta61^{C286,295A/KA}$ that are defective in association with lipid rafts and in inducing lipid raft reorganization (see Fig. S3 in the supplemental material) failed to induce integrin activation (Fig. 4D).

Src is cotranslocated to lipid rafts through association with CD44 and induces integrin activation. In line with our previous observation that CD44-mediated integrin activation was dependent on Src activity (17), the treatment of Src inhibitor PP2 or expression of the dominant-negative Src(K297D) mutant significantly blocked H-3-induced integrin activation in $AZ521/CD44_S$ cells (Fig. 5A). To further substantiate the role of Src in CD44-mediated integrin activation, *Src* transcription was eliminated in HT29 cells by a lentivirus-based RNA interference technique (Fig. 5B). Pooled clones stably expressing either the shRNA targeted at *Src* or the control scramble shRNA were enriched after puromycin selection. As shown, the introduction of shRNA against *Src* significantly reduced the level of Src in HT29 cells, with a concomitant suppression of OPN-mediated integrin activation, and these changes were not observed in the cells infected with the scramble RNA. Furthermore, reexpression of a functional Src containing wobble mutations within the shRNA-*Src* target sequence into these cells rescued OPN-mediated integrin activation, confirming that inhibition of OPN-mediated integrin activation was due to the knockdown of *Src* and not due to "off-target" effects of shRNA treatment.

As Src is one of the proteins that formed a complex with CD44 in lipid rafts, we examined the distribution of Src activity in the Triton X-100-insoluble fractions in relation to CD44-mediated function (Fig. 5C). As shown, a small portion of Src was associated with CD44 in unstimulated cells. Engagement of CD44 significantly enhanced the association of Src with CD44 in both the Triton X-100-soluble and -insoluble fractions. Notably, MβCD treatment that abrogated CD44-mediated integrin activation was associated with a concurrent loss of CD44-associated Src in the raft fraction, whereas Src activity associated with CD44 in the non-raft fraction was hardly affected. Src has been shown to interact with CD44 mediated through the C-terminal tail between aa 304 and aa 318 (44). In agreement, we showed that $CD44_S\Delta37^{C286,295A}$ was in complex with Src, whereas $CD44_S\Delta61^{C286,295A}$, $CD44_S\Delta61^{C286,295A/KA}$, $CD44_S\Delta67^{C286A}$, and $CD44_S\Delta67$ (from which the 15-aa region had been removed) lost the Src interaction (Fig. 5D, top panel). More importantly, engagement of CD44 mutants which were defective in Src interaction failed to promote Src translocation into lipid rafts (Fig. 5D, bottom panel). To verify whether translocation of Src into lipid rafts is dependent on its

samples were then counterstained with anti-raft marker (caveolin-1) Ab and labeled with Alexa 488-conjugated secondary Ab. Representative images taken by confocal laser microscopy are shown. In some experiments, cells were pretreated with 5 μM MβCD for 15 min prior to H-3 MAb or OPN treatment. Image J software (National Institutes of Health) was used to process the immunocytostaining signals of CD44 and raft marker (caveolin-1). The bar graph shows the percentages of colocalized signals in each set of samples expressed as means ± standard deviations. Data are representative of the images of 12 fields derived from each of three independent experiments. **, $P < 0.01$ (*t* test). (B) $AZ521/CD44_{V6-10}$ (top) and HT29 (bottom) cells were pretreated with or without MβCD followed by OPN or H-3 treatment as described above. The whole-cell lysates were prepared and immunoprecipitated (IP) by anti-CD44 H-3 Ab. The immunoprecipitation complexes were subjected to Western blotting (WB) against H-3 and anti-caveolin-1 Ab, respectively. (C) $AZ521/CD44_{V6-10}$ and HT29 cells were incubated in the presence and absence of OPN and H-3 MAb as described in the Fig. 1 legend. The cells were lysed in chilled 1% cold Triton X-100 buffer, and lysates were subjected to sucrose gradient fractionation. A total of 10 fractions were collected from top to bottom, and an equal volume of each fraction was subjected to Western blot analyses for proteins indicated. Fractions 2 to 4 represent the Triton X-100-insoluble raft fraction, and fractions 7 to 10 contain the Triton X-100-soluble cytoplasmic components, including transferrin receptor (TfR). (D) $AZ521/CD44_S$ cells were incubated in the presence of control IgG or H-3 MAb for 1 h. After washing, cells were lysed and Triton X-100-insoluble raft fractions were isolated. The raft fractions were pooled and immunoprecipitated by H-3 MAb. Silver stains of raft proteins (left panel) before immunoprecipitation and those immunoprecipitated by H-3 MAb (right panel) are shown after fractionation by 10% SDS-PAGE. The identities of protein signals identified by mass spectrometry are indicated. (E) Time course of CD44 engagement-induced enrichment of CD44, Src, and integrin β1 into lipid rafts was monitored in $AZ521/CD44_S$ cells. Cells were treated with H-3 MAb or control IgG and harvested at designated time points. Triton X-100-soluble (S) and -insoluble raft (R) fractions were isolated by sucrose gradient fractionation, pooled, and subjected to Western blotting for individual proteins as indicated.
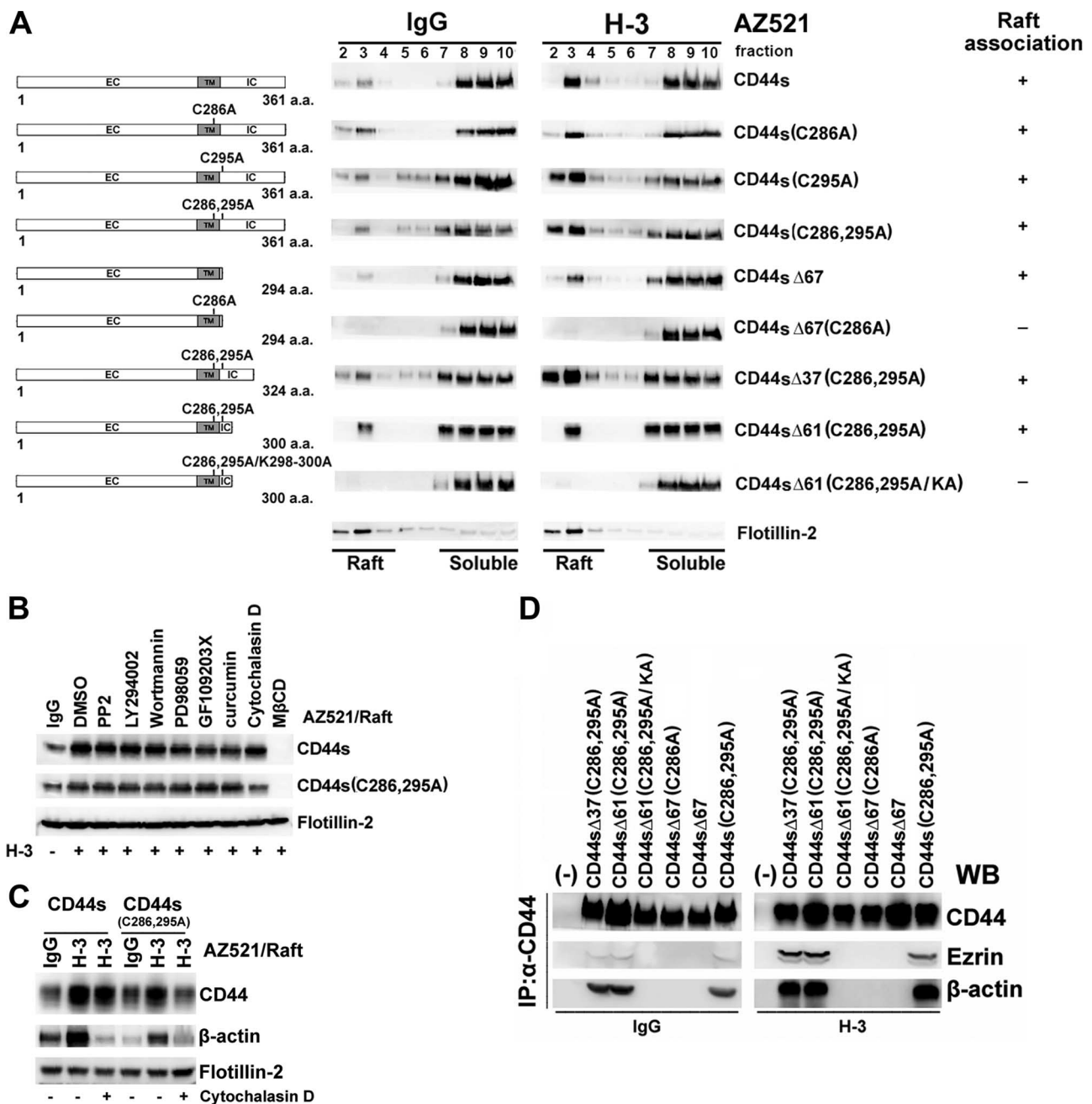
FIG. 3. Both palmitoylation and linkage to the actin cytoskeleton contribute to raft targeting of CD44. Schematic representations of individual CD44 clones are shown at the left. EC, extracellular domain; TM, transmembrane domain; IC, intracellular domain. (A) Individual AZ521/CD44 cell clones were treated with IgG or H-3 MAb as described in the Fig. 1 legend. The cells were lysed in chilled 1% cold Triton X-100 buffer, and lysates were subjected to sucrose gradient fractionation. Engagement-induced association of CD44 to lipid rafts was monitored by Western blot analysis of CD44 in each fraction. The results are summarized at the right: +, association; −, no association. (B) Signaling pathways affecting CD44 raft targeting were examined by pretreating AZ521/CD44$_S$ and AZ521/CD44$_S$^{C286,295A} cell clones with PP2 (30 μM), LY294002 (50 μM), wortmannin (1 μM), PD98059 (50 μM), GF109203X (5 μM), curcumin (5 μM), or vehicle for 30 min or with cytochalasin D (10 μM) for 2 h followed by the treatment of H-3 MAb or IgG. Triton X-100-insoluble raft fractions were isolated, and the presence of CD44 in raft fractions was monitored by Western blotting. DMSO, dimethyl sulfoxide. (C) The association of CD44 and actin in lipid rafts upon H-3 MAb treatment was examined in AZ521/CD44$_S$ and AZ521/CD44$_S$^{C286,295A} cells. Cells were incubated in the presence and absence of cytochalasin D, followed by H-3 MAb or IgG treatment. Raft fractions were isolated and examined by Western blotting for the presence of CD44, actin, and flotillin-2. (D) Association of CD44 with ezrin and actin was examined in AZ521 cells expressing various CD44 clones. After IgG or H-3 MAb treatment, the individual CD44-expressing AZ521 cell clones were lysed. Immunoprecipitation (IP) of total cell lysates by H-3 MAb was performed, followed by fractionation of immunoprecipitates by SDS-PAGE. WB, Western blotting.
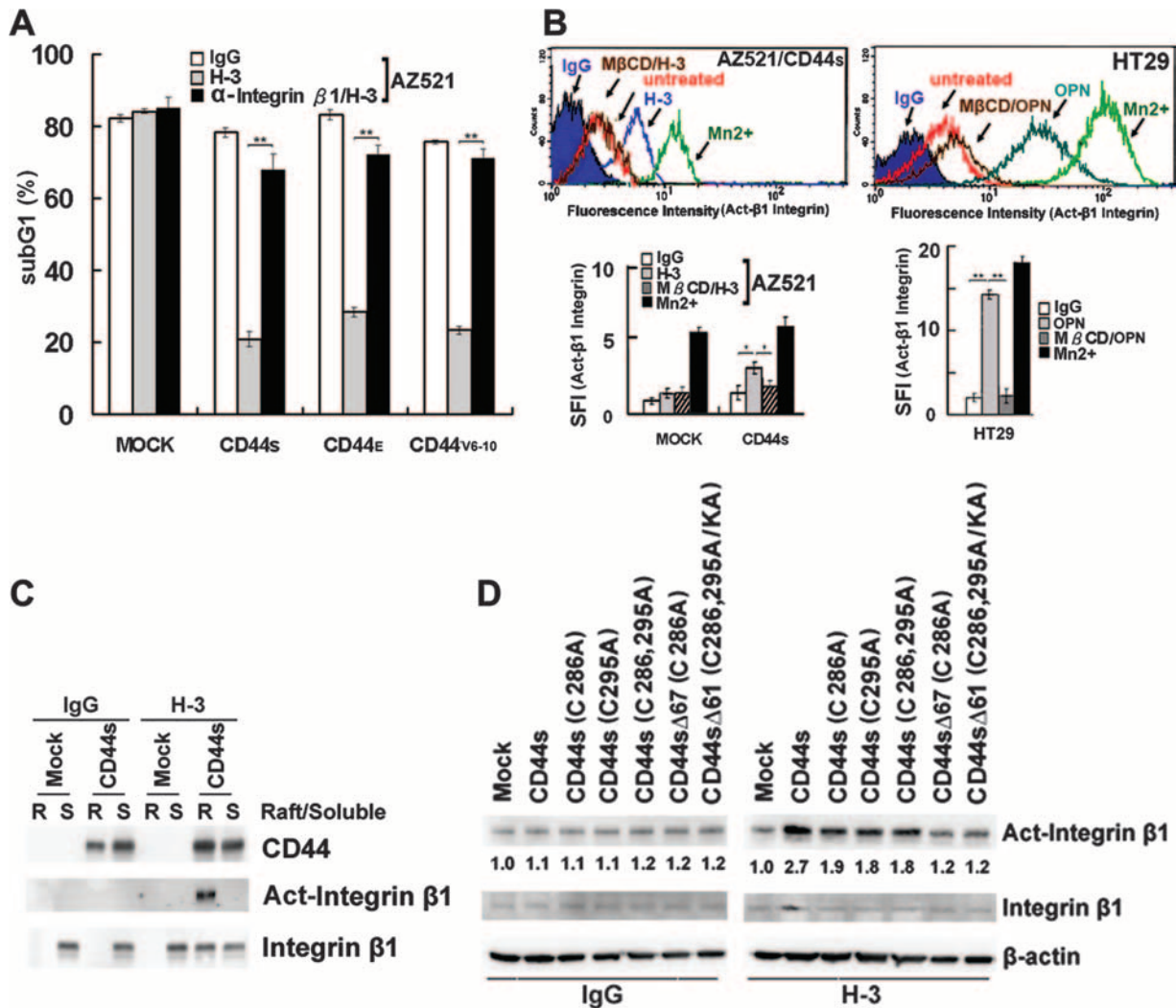
FIG. 4. CD44-mediated survival signal is dependent on integrin activation in lipid rafts. (A) AZ521/Mock and various AZ521/CD44 cell clones were treated with H-3 MAb or control IgG in the presence and absence of blocking Ab against integrin β1, followed by UV irradiation, and apoptosis was measured by flow cytometric analysis of sub-G_1 fractions as described in Materials and Methods. (B) AZ521/Mock, AZ521/CD44$_S$, and HT29 cells were incubated without (untreated) and with H-3 MAb or OPN as described in the Fig. 1 legend. After fixation, cells were stained with MAb against integrin β1 (HUTS-21) or an isotype IgG, labeled with Alexa 488-conjugated secondary Ab, and subjected to flow cytometric analysis. Cells incubated with 2 mM $MnCl_2$ for 30 min at 37°C were included to serve as a positive control. In some experiments, cells were pretreated with 5 mM MβCD for 15 min prior to H-3 MAb treatment. In the histograms, the y axis represents the cell numbers that were stained with Abs in each logarithmic scale of fluorescence amplifier. Similar results were obtained from three independent experiments, and a representative histogram is shown. The specific fluorescence index (SFI) was calculated as the ratio of the mean fluorescence value obtained with the specific Ab and the isotype control Ab. Data from three separate experiments are presented as means ± standard deviations in the bar graph. (C and D) Integrin activation upon engagement of CD44. AZ521/Mock and individual AZ521/CD44$_S$ cell clones were incubated with H-3 MAb or control IgG for 1 h. In panel C, Triton X-100-soluble (S) and -insoluble raft (R) fractions were isolated, followed by Western blot analyses of CD44, integrin β1, and activated integrin β1. In panel D, total cell lysates were prepared and subjected to Western blot analysis of activated integrin β1.

interaction with CD44, a cotransfection experiment was performed to express both the raft-associating CD44$_S$Δ37^{C286,295A} (capable of interacting with Src) and CD44$_S$Δ61^{C286,295A} (incapable of interacting with Src) in various combinations in AZ521 cells (Fig. 5E). Comparable levels of CD44 were detected in lipid rafts, as the total amounts of CD44 to be expressed were kept the same. Increased amounts of Src were detected in the raft fractions along with the increasing amounts of CD44$_S$Δ37^{C286,295A} expressed in the cells, confirming that Src was cotranslocated to lipid rafts through its interaction with CD44. Most importantly, a concurrent increase in integrin

activation was observed, demonstrating that CD44 engagement-induced integrin activation is dependent on the activity of raft-residing Src. We also found that recruitment of integrins in lipid rafts was tightly coupled to CD44-mediated raft reorganization. Upon engagement of CD44 isoforms that were proficient in raft targeting, integrins were detected in Triton X-100-insoluble fractions and remained in complex with CD44; however, engagement of CD44 cells that were defective in raft targeting failed to promote the enrichment of integrins in lipid rafts (Fig. 5D). In line with the fact that CD44-elicited integrin activation is dependent on Src activity in lipid rafts and
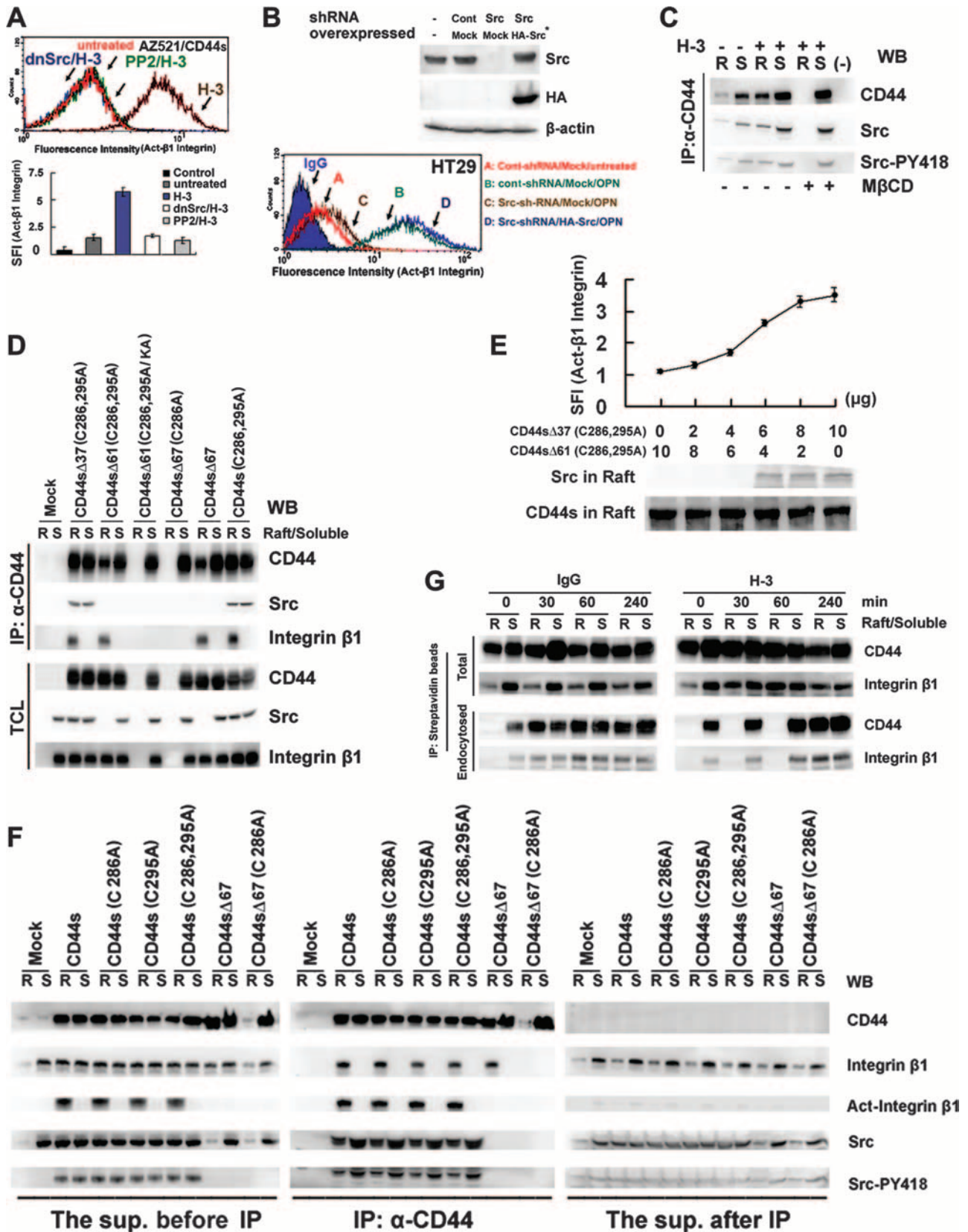
FIG. 5. Src is cotranslocated to lipid rafts through its association with CD44 and induces integrin activation. (A) Activation of integrin β1 was monitored by flow cytometric analyses in control IgG-treated (untreated) or H-3-treated AZ521/CD44$_s$ cells that were pretreated with or without PP2 (30 μM) for 2 h or were transfected with a plasmid encoding dn-Src(K297D). CD44 engagement-mediated integrin activation was measured as

Src depends on CD44 association to be translocated into rafts, integrins are in their active configuration in the raft fractions when being associated in complex with both CD44 and Src (Fig. 5F). When present in the Triton X-100-soluble fractions or present in the raft fractions in the absence of Src, integrins were not activated. In adherent cells, active integrin signaling has been reported to prevent the internalization of caveolae-containing lipid rafts (5). We also showed that CD44 engagement-induced integrin activation was associated with a temporal inhibition of the internalization of raft-associated CD44 and integrins through endocytosis (Fig. 5G).

Raft-dependent CD44-Src-integrin signaling axis promotes cell adherence and enhances matrix-derived survival. Signaling events controlled by integrins regulate important biological processes, such as cell adhesion and survival. As shown, engagement of CD44 conferred increased adherence to FN in AZ521 cells that ectopically expressed CD44 (including $CD44_S$, $CD44_E$, and $CD44_{V6-10}$) but not in AZ521/Mock cells (Fig. 6A). In agreement with the fact that the increased adhesion was mediated through integrin activation, pretreatment of cells with blocking Ab against integrin β1 significantly suppressed CD44-elicited cell adhesion (Fig. 6A). In line with the fact that Src activity is required for CD44-mediated integrin activation, CD44-elicited cell adhesion was repressed in the temperature sensitive v-Src MDCK cells upon shifting from 37°C to 40.5°C (Fig. 6B). Consistent with the notion that lipid raft reorganization was a prerequisite for CD44-mediated integrin activation, CD44-elicited adherence was completely abolished by the treatment of MβCD (Fig. 6C). Conceivably, engagement of CD44 mutants that are defective in Src binding or in raft association would fail to promote cell adhesion (Fig. 6D). FAK is known to transduce integrin-mediated signal derived from ECM. As shown, a concomitant increase in FAK autophosphorylation was observed in the CD44-expressing but not the mock-transfected cells (Fig. 6E), and blockage of matrix-derived signals by transfection and expression of the dominant-negative FAK(Y397F) completely blocked the CD44-mediated, anti-apoptotic response (Fig. 6F). In line with the

observation that CD44-mediated survival was significantly suppressed by MβCD treatment (Fig. 1D), engagement of CD44 mutants defective in Src binding or in raft association also failed to provide cells a survival advantage (Fig. 6G). We therefore conclude that engagement of CD44 confers cells an increased survival propagated from matrix-derived signal transduced by integrins activated through lipid raft reorganization.

DISCUSSION

The cell surface CD44 glycoproteins bind to HA and other glycosaminoglycans and mediate cell adhesion to and migration through ECM. Through its interaction with proteins that bind to the actin microfilaments (7), CD44 serves as a linkage to transmit signal from the cell surface to the cytoplasm. In many of these events, engagement of CD44 induces lipid raft reorganization, which has been suggested to promote the formation of specialized membrane microdomains with multiple signaling molecules assembled in complexes within the vicinity to ensure efficient transduction of sustained signals (7, 9, 13, 25). We have previously shown that OPN-induced engagement of $CD44_V$ confers to cells an increased matrix survival signal mediated through integrin activation (17). In this study, we provide evidence to demonstrate that lipid raft reorganization plays an essential role in CD44-mediated integrin activation, leading to increased survival. We show that engagement of cell surface receptor CD44 induces lipid raft coalescence in several cell types. The lateral reorganization of lipids and membrane-associated proteins promotes the enrichment of CD44, Src, and integrins in lipid rafts, conferring to cells increased adhesion and elevated matrix-derived survival through the lipid raft-associated CD44-Src-integrin signal axis.

Engagement of CD44 induces lipid raft reorganization. It was initially observed by immunofluorescence microscopy that a significantly higher percentage of CD44 was found to be colocalized with lipid raft marker caveolin-1 after engagement, with an increase from 4 to 25% in $AZ521/CD44_S$ and from 22

---

described in the legend for Fig. 4B. (B) HT29 cells were infected with a lentivirus encoding a shRNA targeting Src, shRNA^{Src}, or a control scramble shRNA, shRNA^{Cont}, and cell clones stably harboring shRNA^{Src} and shRNA^{Cont} were obtained after puromycin selection. The stable cell clones were transfected with a control plasmid (Mock) or a plasmid encoding an HA epitope-tagged Src wobble mutant (Src*). Western blotting was performed to measure the expression of Src. Activation of integrin β1 was monitored after OPN treatment for 1 h. (C) Triton X-100-soluble (S) and -insoluble raft (R) fractions were isolated from H-3- and control IgG-treated $AZ521/CD44_S$ cells that were pretreated with or without MβCD. The Triton X-100-soluble and -insoluble raft fractions were pooled and immunoprecipitated (IP) by H-3 MAb or control IgG (−). Western blot (WB) analyses of CD44-associated Src and phosphorylated Src are shown. (D) The Triton X-100-soluble and -insoluble raft fractions were isolated from the individual AZ521/CD44 cell clones as described in the Fig. 1 legend and immunoprecipitated with H-3 MAb. Western blot analyses of CD44, Src, and integrin β1 in detergent-soluble (S) and -insoluble fractions (R) before immunoprecipitation and in the immunoprecipitates were performed. (E) Integrin activation and translocation of Src into lipid rafts were monitored in AZ521 cells cotransfected with plasmids expressing $CD44_S\Delta37^{C286,295A}$ and $CD44_S\Delta61^{C286,295A}$ in various combinations as indicated. Activation of integrin β1 was monitored by flow cytometric analysis as described above. Triton X-100-insoluble fractions were isolated and subjected to Western blotting for CD44 and Src. (F) AZ521/Mock and individual $AZ521/CD44_S$ cell clones were treated with H-3 MAb. Triton X-100-soluble (S) and -insoluble raft (R) fractions were isolated, pooled, and immunoprecipitated with H-3 MAb. Western blot analyses of CD44, Src, Src-pY418, integrin β1, and activated integrin β1 in the raft (R) and Triton X-100-soluble (S) fractions before immunoprecipitation (left panel), in the immunoprecipitates (middle panel), and in the supernatant (right panel) recovered after immunoprecipitation were performed, and enhanced chemiluminescence signal intensity for each probe was recorded simultaneously for the three panels. (G) $AZ521/CD44_S$ cells were labeled with biotin at 4°C, followed by further incubation with control IgG or H-3 MAb at 37°C. At time zero and 30, 60, and 240 min, cells were harvested and Triton X-100-soluble (S) and -insoluble raft (R) fractions were isolated. Biotinylated proteins in the Triton X-100-soluble and -insoluble raft fractions were precipitated using streptavidin beads, and the amounts of CD44 and integrin β1 bound to the beads were determined by Western blot analysis. To examine the internalized receptors, cells were removed to 4°C and incubated in 0.1 M glycine for an additional 30 min prior to the isolation of Triton X-100-soluble and -insoluble raft fractions followed by Western blot analysis of precipitates pulled down by streptavidin beads as described in Materials and Methods.
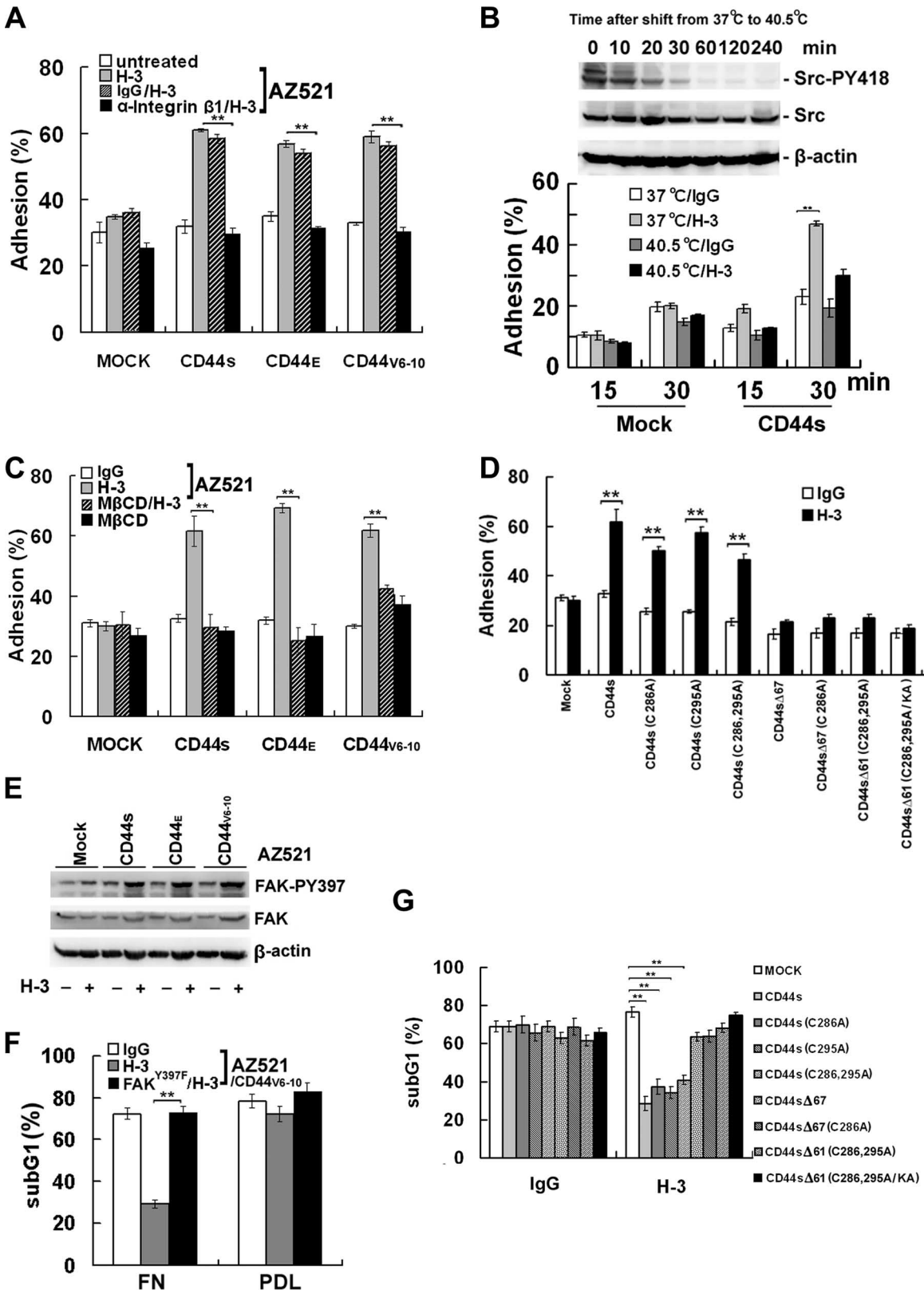
FIG. 6. Raft-dependent CD44-Src-integrin signaling axis promotes cell adherence and matrix-derived survival. (A) Cell adhesion to FN. AZ521/Mock and individual AZ521/CD44 cell clones were trypsinized and treated with H-3 MAb in the presence of blocking Ab against integrin β1 or the control IgG in suspension for 1 h, followed by replating of the cells on FN-coated dishes for 30 min for the adhesion assay. (B) Adhesion of temperature-sensitive v-Src MDCK cells to FN upon temperature shift. The temperature-sensitive v-Src-transformed MDCK cells were transfected with a control plasmid or the plasmid encoding human CD44$_S$ and grown at permissive (37°C) temperature. Cells were then shifted

to 60% in HT29 cells (Fig. 2A and B), and that the colocalization was greatly inhibited by treating cells with MβCD or nystatin. CD44 engagement-induced lateral reorganization of membrane-associated proteins was further demonstrated by the isolation and characterization of lipid rafts by sucrose gradient centrifugation of cold-detergent-extracted cell lysates. Despite the fact that lipid rafts are suggested to have half-lives less than 100 nanoseconds, a 2.5- to 3-fold increase in protein level was recovered from the low-density buoyant raft fractions from stimulated cells. Upon engagement of CD44, a variety of proteins were enriched in the low-density raft fraction, including CD44, Src, and integrin β1 (Fig. 2D and E). Recent studies have indicated that many proteins are palmitoylated and/or tend to form oligomers, which facilitate the incorporation in lipid raft-like microenvironments. In agreement with this, we showed that palmitoylation of the membrane-proximal cysteine residues contributes to raft association of CD44. Nevertheless, removal of these cysteine residues was not sufficient to prevent CD44 from raft association. It was only when both the cytoplasmic domain and the membrane-proximal cysteine residues were removed that CD44 became completely excluded from the raft fraction, suggesting that C-terminal linkage to the actin cytoskeleton through protein-protein interactions also contributes to the association of CD44 with lipid rafts.

The major theme demonstrated in this study is that lipid raft reorganization plays an essential role in assembling the CD44-Src-integrin signaling axis to facilitate cell survival. This was established based on the observations that CD44-mediated integrin activation was detected only in lipid rafts (Fig. 4C and 5F) and that integrin activation was tightly coupled to Src that was recruited to lipid rafts by CD44 (Fig. 5E). Initially, we demonstrated that CD44 engagement promotes the lateral movement of CD44, Src, and integrins into lipid rafts (Fig. 2E). By expressing various CD44 mutants in CD44-null human gastric AZ521 cells, we showed that Src was cotranslocated to lipid rafts through its association with CD44, as demonstrated by the fact that the level of Src translocated to lipid rafts was correlated to the level of raft-associated CD44 that was capable of interacting with Src (Fig. 5D and E). Engagement of CD44 mutants devoid of an intact Src-binding site failed to induce the translocation of Src into lipid rafts (Fig. 5D and F). Our data also showed that CD44-elicited enrichment of integrins in lipid rafts was tightly associated with the translocation of CD44 into lipid rafts (Fig. 5D and F). Although the mechanism through which integrins are relocalized to lipid rafts upon CD44 engagement is still not clear, our data clearly indicate that integrins and Src are recruited to lipid rafts by CD44 through different mechanisms.

Engagement of CD44 leads to the association of clustered receptors with lipid rafts. We envision that the perturbation of lipid bilayer and membrane proteins during receptor engagement may facilitate the formation of larger raft structures with longer half-lives, in a way similar to that described in T-cell immunological synapses (8). One possible mechanism is through the transient suppression of the internalization of lipid rafts. Local activation of integrin has been proposed to suppress the internalization of lipid rafts (5). Similarly, we showed that engagement of CD44 promoted the enrichment of CD44 and integrin β1 in lipid rafts, which was associated with a temporal inhibition of the endocytosis process (Fig. 5G). It remains to be determined whether CD44 engagement-induced integrin activation may in part facilitate the formation of CD44 complex in lipid rafts by suppressing the internalization of lipid rafts. It has been suggested that protein-protein interactions, not lipid raft recruitment, may be the main driving force for the assembly of signaling complexes (32). Based on our finding that engagement of CD44 facilitates the assembly of signaling complexes of CD44, Src, and integrins in lipid rafts, we propose that CD44 engagement-induced translocation of proteins into rafts is a selective process and the capacity to remain temporally stable in rafts is a property of only a small number of membrane-associated proteins. In support of this, we showed that both Src and intergin β1 are present in complexes with CD44 in the raft fraction by coimmunoprecipitation and that the recruitment of Src and integrins to lipid rafts is tightly coupled to CD44. Although the selectivity and specificity of proteins to be enriched in lipid rafts are not completely transparent, these processes allow the definition of the precise location and cellular neighbors for specific downstream signaling pathways. We envision that factors that affect these processes would be predicted to have the potential to modulate CD44 signaling.

The Src family kinases (SFKs) are classified as oncogenic proteins due to their ability to activate cell proliferation, spreading, and migration. The interaction between Src kinases and membrane-linked molecules is known to regulate receptor signaling and various cellular functions (30). SFKs have been shown to be coupled to CD44-mediated cellular signaling in T lymphocytes (12, 35) and human prostate (44) and ovarian (2) tumor cells. SFKs are known to be myristoylated at their N termini. Most of them, except Src, Blk, and the p61 isoform of Hck, are also palmitoylated at a nearby Cys residue (14, 15, 26,

---

to nonpermissive (40.5°C) temperature and incubated for the designated times as indicated. Cells were harvested, and Western blot analyses of Src and phosphorylated Src were performed. For the adhesion assay, the transfected cells were grown at permissive (37°C) and nonpermissive (40.5°C) temperatures for pp60^{v-Src} activity for 2 h, transferred to medium containing H-3 MAb or an isotype IgG for 1 h, and replated on FN-coated dishes for 15 and 30 min. (C) Adhesion to FN was monitored in H-3- or control IgG-treated AZ521/Mock and AZ521/CD44 cell clones pretreated with or without 5 mM MβCD. (D) Adhesion to FN was monitored in H-3- or control IgG-treated AZ521 cells expressing the wild-type or designated CD44$_S$ mutant clone. (E) AZ521/Mock and AZ521/CD44 cell clones were incubated with or without H-3 MAb in suspension for 1 h, replated on FN-coated dishes for 30 min, and harvested for Western blot analyses of FAK and phosphorylated FAK. (F) AZ521/CD44$_{V6-10}$ cells were transfected with or without a plasmid encoding FAK^{Y397F}. After 36 h, cells were treated with H-3 MAb in suspension for 1 h, replated on FN or poly-D-lysine (PDL) for 3 h, and subjected to UV irradiation. Apoptotic fractions were measured by flow cytometric analysis after 48 h. (G) UV-induced apoptosis was monitored in H-3- or control IgG-treated AZ521/Mock and various AZ521/CD44$_S$ mutants. Data were derived from three independent experiments and presented as means ± standard deviations. ∗∗, $P < 0.01$ (t test).

33, 43). The dual-acylated SFKs such as Fyn, Lyn, Lck, and Hck p59 are constitutively membrane localized to some extent, and dual acylation is important for the inclusion of these SFKs into lipid rafts of fibroblasts and leukocytes (14, 33, 41). Src is usually recruited to the membrane upon stimulation (4). Whether the monoacylated Src, frequently hyperactive in carcinomas, also localizes at rafts is controversial. Despite the absence of a palmitoylation signal, utilization of Src-specific Ab has demonstrated the recruitment of ligand-stimulated Src to Ephrin B1-containing microdomains in neurons (27) and the association of neuronal Src with brain lipid rafts (21). In these cases, the raft-localized Src was more catalytically active than its counterpart in the soluble fraction (4, 21, 27). These data suggest not only the actual localization of Src to rafts, at least in some tissues, but also the involvement of raft-localized Src in signal transduction. In our study, we showed in Fig. 2E that most of the Src was present in the detergent-soluble fractions in the unstimulated cells and that engagement of CD44 promotes the binding of Src to CD44 with enhanced Src kinase activity (Fig. 5C). By cotransfection and expression of C-terminal CD44 mutants, of which one is competent and the other defective in Src binding in various combinations, we further demonstrated that Src was recruited to lipid rafts through its association with CD44 and was directly involved in stimulating integrin activity (Fig. 5E) and the subsequent integrin-mediated cell functions (Fig. 6B). It remains to be determined whether monoacylation of Src is required for its involvement in CD44-mediated signaling.

In summary, we propose a working hypothesis that engagement of CD44 induces lipid raft reorganization. By linkage to the actin cytoskeleton through linker proteins (ERM proteins), CD44 and its interacting protein Src are relocalized in the reorganized lipid rafts along with many other proteins, including integrins. In these specialized membrane microdomains, CD44-Src is brought within close proximity to integrins and triggers integrin activation. As a consequence, cells expressing CD44 display an increased adherence and elevated matrix survival signal. Therefore, the data suggest that the major functions ascribed to CD44, matrix adhesion, growth promotion, and cell survival, should not be considered separate processes, as they are interconnected through the assembly of CD44 and interacting molecules in lipid rafts.

REFERENCES

1. **Behrens, J., L. Vakaet, R. Friis, E. Winterhager, F. Van Roy, M. M. Mareel, and W. Birchmeier.** 1993. Loss of epithelial differentiation and gain of invasiveness correlates with tyrosine phosphorylation of the E-cadherin/beta-catenin complex in cells transformed with a temperature-sensitive v-SRC gene. J. Cell Biol. **120:**757–766.
2. **Bourguignon, L. Y., H. Zhu, L. Shao, and Y. W. Chen.** 2001. CD44 interaction with c-Src kinase promotes cortactin-mediated cytoskeleton function and hyaluronic acid-dependent ovarian tumor cell migration. J. Biol. Chem. **276:**7327–7336.
3. **Chen, J. Y., W. D. Funk, W. E. Wright, J. W. Shay, and J. D. Minna.** 1993. Heterogeneity of transcriptional activity of mutant p53 proteins and p53 DNA target sequences. Oncogene **8:**2159–2166.
4. **de Diesbach, P., T. Medts, S. Carpentier, L. D'Auria, P. Van Der Smissen, A. Platek, M. Mettlen, A. Caplanusi, M. F. van den Hove, D. Tyteca, and P. J. Courtoy.** 2008. Differential subcellular membrane recruitment of Src may specify its downstream signalling. Exp. Cell Res. **314:**1465–1479.
5. **del Pozo, M. A., N. Balasubramanian, N. B. Alderson, W. B. Kiosses, A. Grande-Garcia, R. G. Anderson, and M. A. Schwartz.** 2005. Phospho-caveolin-1 mediates integrin-regulated membrane domain internalization. Nat. Cell Biol. **7:**901–908.
6. **Dykstra, M., A. Cherukuri, and S. K. Pierce.** 2001. Rafts and synapses in the spatial organization of immune cell signaling receptors. J. Leukoc. Biol. **70:**699–707.
7. **Foger, N., R. Marhaba, and M. Zoller.** 2001. Involvement of CD44 in cytoskeleton rearrangement and raft reorganization in T cells. J. Cell Sci. **114:**1169–1178.
8. **Gaus, K., E. Chklovskaia, B. Fazekas de St. Groth, W. Jessup, and T. Harder.** 2005. Condensation of the plasma membrane at the site of T lymphocyte activation. J. Cell Biol. **171:**121–131.
9. **Ghatak, S., S. Misra, and B. P. Toole.** 2005. Hyaluronan constitutively regulates ErbB2 phosphorylation and signaling complex formation in carcinoma cells. J. Biol. Chem. **280:**8875–8883.
10. **Horejsi, V., K. Drbal, M. Cebecauer, J. Cerny, T. Brdicka, P. Angelisova, and H. Stockinger.** 1999. GPI-microdomains: a role in signalling via immunoreceptors. Immunol. Today **20:**356–361.
11. **Hynes, R. O.** 1992. Integrins: versatility, modulation, and signaling in cell adhesion. Cell **69:**11–25.
12. **Ilangumaran, S., A. Briol, and D. C. Hoessli.** 1998. CD44 selectively associates with active Src family protein tyrosine kinases Lck and Fyn in glycosphingolipid-rich plasma membrane domains of human peripheral blood lymphocytes. Blood **91:**3901–3908.
13. **Ito, T., J. D. Williams, D. Fraser, and A. O. Phillips.** 2004. Hyaluronan attenuates transforming growth factor-beta1-mediated signaling in renal proximal tubular epithelial cells. Am. J. Pathol. **164:**1979–1988.
14. **Janes, P. W., S. C. Ley, and A. I. Magee.** 1999. Aggregation of lipid rafts accompanies signaling via the T cell antigen receptor. J. Cell Biol. **147:**447–461.
15. **Koegl, M., P. Zlatkine, S. C. Ley, S. A. Courtneidge, and A. I. Magee.** 1994. Palmitoylation of multiple Src-family kinases at a homologous N-terminal motif. Biochem. J. **303:**749–753.
16. **Lee, J. L., C. T. Lin, L. L. Chueh, and C. J. Chang.** 2004. Autocrine/paracrine secreted Frizzled-related protein 2 induces cellular resistance to apoptosis: a possible mechanism of mammary tumorigenesis. J. Biol. Chem. **279:**14602–14609.
17. **Lee, J. L., M. J. Wang, P. R. Sudhir, G. D. Chen, C. W. Chi, and J. Y. Chen.** 2007. Osteopontin promotes integrin activation through outside-in and inside-out mechanisms: OPN-CD44V interaction enhances survival in gastrointestinal cancer cells. Cancer Res. **67:**2089–2097.
18. **Legg, J. W., and C. M. Isacke.** 1998. Identification and functional analysis of the ezrin-binding site in the hyaluronan receptor, CD44. Curr. Biol. **8:**705–708.
19. **Liu, D., and M. S. Sy.** 1996. A cysteine residue located in the transmembrane domain of CD44 is important in binding of CD44 to hyaluronic acid. J. Exp. Med. **183:**1987–1994.
20. **Lundell, B. I., J. B. McCarthy, N. L. Kovach, and C. M. Verfaillie.** 1997. Activation of beta1 integrins on CML progenitors reveals cooperation between beta1 integrins and CD44 in the regulation of adhesion and proliferation. Leukemia **11:**822–829.
21. **Mukherjee, A., L. Arnaud, and J. A. Cooper.** 2003. Lipid-dependent recruitment of neuronal Src to lipid rafts in the brain. J. Biol. Chem. **278:**40806–40814.
22. **Nandi, A., P. Estess, and M. Siegelman.** 2004. Bimolecular complex between rolling and firm adhesion receptors required for cell arrest; CD44 association with VLA-4 in T cell extravasation. Immunity **20:**455–465.
23. **Neame, S. J., C. R. Uff, H. Sheikh, S. C. Wheatley, and C. M. Isacke.** 1995. CD44 exhibits a cell type dependent interaction with Triton X-100 insoluble, lipid rich, plasma membrane domains. J. Cell Sci. **108:**3127–3135.
24. **Oliferenko, S., K. Paiha, T. Harder, V. Gerke, C. Schwarzler, H. Schwarz, H. Beug, U. Gunthert, and L. A. Huber.** 1999. Analysis of CD44-containing lipid rafts: recruitment of annexin II and stabilization by the actin cytoskeleton. J. Cell Biol. **146:**843–854.
25. **Orian-Rousseau, V., L. Chen, J. P. Sleeman, P. Herrlich, and H. Ponta.** 2002. CD44 is required for two consecutive steps in HGF/c-Met signaling. Genes Dev. **16:**3074–3086.
26. **Paige, L. A., M. J. Nadler, M. L. Harrison, J. M. Cassady, and R. L. Geahlen.** 1993. Reversible palmitoylation of the protein-tyrosine kinase p56lck. J. Biol. Chem. **268:**8669–8674.
27. **Palmer, A., M. Zimmer, K. S. Erdmann, V. Eulenburg, A. Porthin, R. Heumann, U. Deutsch, and R. Klein.** 2002. EphrinB phosphorylation and reverse signaling: regulation by Src kinases and PTP-BL phosphatase. Mol. Cell **9:**725–737.
28. **Perschl, A., J. Lesley, N. English, R. Hyman, and I. S. Trowbridge.** 1995. Transmembrane domain of CD44 is required for its detergent insolubility in fibroblasts. J. Cell Sci. **108:**1033–1041.

29. **Rangaswami, H., A. Bulbule, and G. C. Kundu.** 2006. Osteopontin: role in cell signaling and cancer progression. Trends Cell Biol. **16:**79–87.

30. **Schlessinger, J.** 2000. New roles for Src kinases in control of cell survival and angiogenesis. Cell **100:**293–296.

31. **Screaton, G. R., M. V. Bell, D. G. Jackson, F. B. Cornelis, U. Gerth, and J. I. Bell.** 1992. Genomic structure of DNA encoding the lymphocyte homing receptor CD44 reveals at least 12 alternatively spliced exons. Proc. Natl. Acad. Sci. USA **89:**12160–12164.

32. **Shaw, A. S.** 2006. Lipid rafts: now you see them, now you don't. Nat. Immunol. **7:**1139–1142.

33. **Shenoy-Scaria, A. M., D. J. Dietzen, J. Kwong, D. C. Link, and D. M. Lublin.** 1994. Cysteine3 of Src family protein tyrosine kinase determines palmitoylation and localization in caveolae. J. Cell Biol. **126:**353–363.

34. **Sherman, L. S., T. A. Rizvi, S. Karyala, and N. Ratner.** 2000. CD44 enhances neuregulin signaling by Schwann cells. J. Cell Biol. **150:**1071–1084.

35. **Taher, T. E., L. Smit, A. W. Griffioen, E. J. Schilder-Tol, J. Borst, and S. T. Pals.** 1996. Signaling through CD44 is mediated by tyrosine kinases. Association with p56lck in T lymphocytes. J. Biol. Chem. **271:**2863–2867.

36. **Thankamony, S. P., and W. Knudson.** 2006. Acylation of CD44 and its association with lipid rafts are required for receptor and hyaluronan endocytosis. J. Biol. Chem. **281:**34601–34609.

37. **Tsukita, S., K. Oishi, N. Sato, J. Sagara, A. Kawai, and S. Tsukita.** 1994.

38. **van Meer, G.** 2005. Cellular lipidomics. EMBO J. **24:**3159–3165.

39. **von Haller, P. D., S. Donohoe, D. R. Goodlett, R. Aebersold, and J. D. Watts.** 2001. Mass spectrometric characterization of proteins extracted from Jurkat T cell detergent-resistant membrane domains. Proteomics **1:**1010–1021.

40. **Wang, H. S., Y. Hung, C. H. Su, S. T. Peng, Y. J. Guo, M. C. Lai, C. Y. Liu, and J. W. Hsu.** 2005. CD44 cross-linking induces integrin-mediated adhesion and transendothelial migration in breast cancer cell line by up-regulation of LFA-1 (alpha L beta2) and VLA-4 (alpha4beta1). Exp. Cell Res. **304:**116–126.

41. **Wolven, A., H. Okamura, Y. Rosenblatt, and M. D. Resh.** 1997. Palmitoylation of p59fyn is reversible and sufficient for plasma membrane association. Mol. Biol. Cell **8:**1159–1173.

42. **Yu, W. H., J. F. Woessner, Jr., J. D. McNeish, and I. Stamenkovic.** 2002. CD44 anchors the assembly of matrilysin/MMP-7 with heparin-binding epidermal growth factor precursor and ErbB4 and regulates female reproductive organ remodeling. Genes Dev. **16:**307–323.

43. **Yurchak, L. K., and B. M. Sefton.** 1995. Palmitoylation of either Cys-3 or Cys-5 is required for the biological activity of the Lck tyrosine protein kinase. Mol. Cell. Biol. **15:**6914–6922.

44. **Zhu, D., and L. Y. Bourguignon.** 1998. The ankyrin-binding domain of CD44s is involved in regulating hyaluronic acid-mediated functions and prostate tumor cell transformation. Cell Motil. Cytoskeleton **39:**209–222.

ERM family members as molecular linkers between the cell surface glycoprotein CD44 and actin-based cytoskeletons. J. Cell Biol. **126:**391–401.